Anal. Chem. **2010,** *82,* 7842–7848

4D Shearforce-Based Constant-Distance Mode Scanning Electrochemical Microscopy

Michaela Nebel,[†] Kathrin Eckhard,[†] Thomas Erichsen,[‡] Albert Schulte,[§] and Wolfgang Schuhmann*,[†]

Analytische Chemie−Elektroanalytik and Sensorik, Ruhr-Universität Bochum, Universitätsstrasse 150, 44780 Bochum, Germany, Sensolytics GmbH, Universitätsstrasse 142, 44799 Bochum, Germany, and Biochemistry-Electrochemistry Research Unit, School of Chemistry and Biochemistry, Institute of Science, Suranaree University of Technology, Nakhon Ratchasima 30000, Thailand

4D shearforce-based constant-distance mode scanning electrochemical microscopy (4D SF/CD-SECM) is designed to assess SECM tip currents at several but constant distances to the sample topography at each point of the *x*,*y*-scanning grid. The distance dependent signal is achieved by a shearforce interaction between the in-resonance vibrating SECM tip and the sample surface. A 4D SF/CD-SECM measuring cycle at each grid point involves a shearforce controlled SECM tip *z*-approach to a point of closest distance and subsequent stepwise tip retractions. At the point of closest approach and during the retraction steps, pairs of tip current (*I*) and position are acquired for various distances above the sample surface. Such a sequence provides *x*,*y*,*I* maps, that can be compiled and displayed for each selected data acquisition distance. Thus, multiple SECM images are obtained at known and constant distances above the sample topography. 4D SF/CD-SECM supports distance-controlled tip operation while continuous scanning of the SECM tip in the shear-force distance is avoided. In this way, constant-distance mode SECM imaging can be performed at user-defined, large tip-to-sample distances. The feasibility and the potential of the proposed 4D SF/CD-SECM imaging is demonstrated using on the one hand amperometric feedback mode imaging of a Pt band electrode array and on the other hand the visualization of the diffusion zone of a redox active species above a microelectrode in a generator/collector arrangement.

Scanning electrochemical microscopy[1] (SECM) is a powerful electrochemical imaging technique with an application range from materials to life science. SECM visualizes the topography and/or the local chemical reactivity based on the highly localized current response of an ultramicroelectrode (UME) that is scanned as the SECM tip in close proximity over a predefined area of the sample. Initially, SECM imaging employed disk-shaped UMEs with about 5−25 μm diameter and the negative/positive feedback or the generator/collector mode of detection. Tip movements were performed in a scanning plane at a fixed displacement of the *z*-positioning element in close proximity above the sample surface (constant-height mode). However, as recently reviewed,[2−7] a significant progress in the application of SECM has been achieved such as the successful operation of smaller SECM tips and the implementation of alternative detection modes instead of tip amperometry. Furthermore, the integration of advanced positioning devices and strategies and the establishment of novel scanning and detection modes for a better 3D contour profiling together with an improved specificity and sensitivity have been accomplished.

The application of smaller electrodes made the constant-distance positioning a requirement in order to avoid tip crash, loss of near-field interaction, or an undefined impact of sample topography. This was previously achieved, among other strategies, by the integration of a constant-distance mode into SECM mainly using shearforce range interactions between an in resonance vibrating tip and the sample surface.[8−16] Existing shearforce-based distance control strategies are using the continuous optical,[8,10,13] piezoelectric,[11] or tuning fork[9,12,14] detection of the amplitude of the vibrating SECM tip as input for the feedback loop that keeps

* To whom correspondence should be addressed. E-mail: wolfgang.schuhmann@rub.de. Phone: +492343226200. Fax: +492343214683.

[†] Ruhr-Universität Bochum.

[‡] Sensolytics GmbH.

[§] Suranaree University of Technology.

(1) Bard, A. J.; Mirkin, M. V., Eds. *Scanning electrochemical microscopy*; John Wiley and Sons: New York, 2001.

(2) Wittstock, G.; Burchardt, M.; Pust, S. E.; Shen, Y.; Zhao, C. *Angew. Chem., Int. Ed.* **2007**, *46*, 1584–1617.

(3) Schulte, A.; Schuhmann, W. *Angew. Chem., Int. Ed.* **2007**, *46*, 8760–8777.

(4) Sun, P.; Laforge, F. O.; Mirkin, M. V. *Phys. Chem. Chem. Phys.* **2007**, *9*, 802–823.

(5) Szunerits, S.; Pust, S. E.; Wittstock, G. *Anal. Bioanal. Chem.* **2007**, *389*, 1103–1120.

(6) Stoica, L.; Neugebauer, S.; Schuhmann, W. *Adv. Biochem. Eng./Biotechnol.* **2008**, *109*, 455–492.

(7) Amemiya, S.; Bard, A. J.; Fan, F. R. F.; Mirkin, M. V.; Unwin, P. R. *Ann. Rev. Anal. Chem.* **2008**, *1*, 95–131.

(8) Ludwig, M.; Kranz, C.; Schuhmann, W.; Gaub, H. E. *Rev. Sci. Instrum.* **1995**, *66*, 2857–2860.

(9) James, P. I.; Garfias-Mesias, L. F.; Moyer, P. J.; Smyrl, W. H. *J. Electrochem. Soc.* **1998**, *145*, L64–L66.

(10) Hengstenberg, A.; Kranz, C.; Schuhmann, W. *Chem.—Eur. J.* **2000**, *6*, 1547–1554.

(11) Ballesteros Katemann, B.; Schulte, A.; Schuhmann, W. *Chem.—Eur. J.* **2003**, *9*, 2025–2033.

(12) Oyamatsu, D.; Hirano, Y.; Kanaya, N.; Mase, Y.; Nishizawa, M.; Matsue, T. *Bioelectrochemistry* **2003**, *60*, 115–121.

(13) Pitta Bauermann, L.; Schuhmann, W.; Schulte, A. *Phys. Chem. Chem. Phys.* **2004**, *6*, 4003–4008.

(14) Yamada, H.; Fukumoto, H.; Yokoyama, T.; Koike, T. *Anal. Chem.* **2005**, *77*, 1785–1790.

(15) Hengstenberg, A.; Blöchl, A.; Dietzel, I. D.; Schuhmann, W. *Angew. Chem., Int. Ed.* **2001**, *40*, 905–909.

(16) Isik, S.; Schuhmann, W. *Angew. Chem., Int. Ed.* **2006**, *44*, 7451–7454.

10.1021/ac1008805
Published on Web 08/25/2010

the tip-to-surface separation constant throughout scanning. Very near to the surface, short-range hydrodynamic shearforces obstruct the free lateral tip motion. The shearforce interactions extend to distances of a maximum of a few hundred nanometers. Regardless of the type of the shearforce detection, lateral tip movement at a fixed degree of damping equals a noncontact scanning in constant tip-to-sample distance in the regime of the shearforce interaction, e.g., at extremely small distances between tip and sample. In addition to acquiring the sample topography, there are several advantages of a shearforce-supported SECM tip guidance. First, tip crash is avoided when scanning tilted sample surfaces and 3D objects, respectively. Second, the electrochemical information given by the locally recorded tip current is no longer falsified by artifacts due to the sample topography. Despite that shearforce-based constant-distance positioning was used in a number of studies and opened the route for securely applying nanoelectrodes as SECM tips, the shearforce-assisted constant-distance mode has shortcomings, too. Mapping of larger areas in reasonable time is hardly possible due to the fact that the scan speed is limited by allowing the feedback loop to be reestablished to or at least within a certain range of the set-point value of damping of tip vibration. However, most importantly, no information at tip-to-sample distances outside the range of the shearforce interaction can be obtained in the conventional constant-distance mode. Recently, the standing approach (STA) mode of SECM was suggested as a strategy to circumvent some of the inherent problems related to an extremely close positioning distance in the shearforce mode on soft samples.[17,18] In order to collect additional local properties at particular grid points of an *x,y* plane, than just the mere amperometric tip response, one was led to use sophisticated measuring procedures for multiparameter SECM imaging. The development of special scanning probes and/or the implementation of tailored hard- and software have enabled a point-by-point acquisition of full impedance spectra,[19] complete fast scan cyclic[20] or anodic stripping[21,22] voltammograms, and associated electrochemical or optical data.[5]

Here, we describe the development of a 4D shearforce-based constant-distance mode of SECM (4D SF/CD-SECM) as a more general approach which allows an electrochemical imaging at predefined and constant distances above the sample topography. The principles and technical details of this approach are outlined and discussed. The feasibility is demonstrated by a 4D imaging of the feedback regime of a Pt band microelectrode array and of the distance-dependent diffusion profile of redox active species that evolve in front of the electroactive area of a disk-shaped electrode using the generator/collector mode of SECM.

EXPERIMENTAL SECTION

Chemicals and Materials. All chemicals were used as received without further purification. Aqueous solutions were prepared using Milli-Q water. $[Ru(NH_3)_6]Cl_3$ was purchased from ABCR (Karlsruhe, Germany), and KCl was from Riedel-de Haën (Seelze, Germany). An electrolyte containing 5 mM $[Ru(NH_3)_6]^{3+}$ and 100 mM KCl was used for all SECM experiments. Materials for the electrode preparation comprise borosilicate glass capillaries (length 100 mm, outside Ø 1.5 mm, inside Ø 0.75 mm) from Hilgenberg (Malsfeld, Germany), straight pieces of copper wires (Ø 0.5 mm), carbon cement from Plano (Wetzlar, Germany), and carbon fibers of the type Grafil E/XA-S (Ø ≈ 7−9 μm) from Courtaulds Limited Carbon Fibres Division (Coventry, United Kingdom). For surface cleaning, the supplied multiple-filament strands of carbon fibers were soaked for 24 h in acetone, rinsed with distilled water, and dried. The cathodic electrodeposition paint FREIOTHERM-Electrocoating, KTL "automotive upgrade" was used for carbon fiber insulation and obtained from FreiLacke (Bräunlingen, Germany).

SECM Tip and Sample Preparation. Polymer-insulated disk-shaped carbon fiber UMEs served as vibrationable SECM tips for the shearforce-mode experiments. They were fabricated following a previously published routine.[13] In brief, a single carbon fiber was attached to a copper wire with carbon cement used as conductive glue. The carbon fiber/copper wire assembly was then threaded into a glass capillary and fixed in there with a tiny drop of a standard two-component epoxy resin. The glass capillary with the carbon fiber inside was pulled with a homemade glass pipet puller in such a way that the carbon fiber extended well beyond the end of the produced glass tip. Special care was taken that a watertight glass/carbon junction and a straight-tapered long-pulled glass section were obtained. The latter is important to get SECM tips with a sufficiently good flexibility to support the oscillation at an adequate resonance frequency for shearforce detection. The extending bare carbon fiber was finally insulated by a cathodic electrodeposition paint. For the precipitation of a thin layer of the electrodeposition paint, a constant voltage of 10 V was applied for 5 min between the carbon fiber cathode and a Pt ring counter electrode. Freshly electropainted electrodes were heat cured in an oven for 20 min at 180 °C and stored until further used. Prior to a SECM experiment, scalpel cutting perpendicular to the fiber axes exposed a fresh disk-shaped carbon surface of about 7−9 μm diameter. Cyclic voltammetry in a $[Ru(NH_3)_6]^{3+}$-containing electrolyte was performed to inspect the quality of the carbon surface and insulation. Carbon fiber microelectrodes used as SECM tips need to display a well-pronounced sigmoidal I/E curve in the cyclic voltammogram.

One of the samples inspected in this study with 4D SF/CD-SECM was kindly provided by Prof. Milena Koudelka, University of Neuchâtel, CH, comprising an array of four parallel Pt microband electrodes, each of them about 1 μm in height, 1 mm in length, 25 μm in width, and with 25 μm insulating space between them. The second sample was a smoothly polished 100 μm diameter Pt disk electrode that was embedded in a planar insulating glass sheath of several millimeter diameter.

SECM Instrumentation. All SECM experiments were performed with a setup that was similar to an earlier described version.[10,13] For the operation of the shearforce-based constant-distance mode with an optical detection of shearforces between the SECM tip and the sample, the setup consisted of the following

(17) Maruyama, K.; Ohkawa, H.; Ogawa, S.; Ueda, A.; Niwa, O.; Suzuki, K. *Anal. Chem.* **2006**, *78*, 1904–1912.
(18) Yamada, H.; Fukumoto, H.; Yokoyama, T.; Koike, T. *Anal. Chem.* **2005**, *77*, 1785–1790.
(19) Eckhard, K.; Erichsen, T.; Stratmann, M.; Schuhmann, W. *Chem.—Eur. J.* **2008**, *14*, 3968–3976.
(20) Schrock, D. S.; Baur, J. E. *Anal. Chem.* **2007**, *79*, 7053–7061.
(21) Daniele, S.; Ciani, I.; Bragato, C.; Baldo, M. A. *J. Phys. IV* **2003**, *107*, 353–356.
(22) Alpuche-Aviles, M. A.; Baur, J. E.; Wipf, D. O. *Anal. Chem.* **2008**, *80*, 3612–3621.

components: a piezoelectric tube (PSt 150/4/20, Piezomechanik Pickelmann, München, Germany) for tip agitation, a function generator (HP 33120A, Hewlett-Packard, USA) as source of the sinusoidal piezo agitation voltage, a Laser (LDM-5-635-1, Optronics, Kehl, Germany) able to provide a precisely focused beam, a split photodiode (Spot 4D, laser2000, Wessling, Germany) for optoelectronic signal detection, and a lock-in amplifier (Model 7280, Signal Recovery, Wokingham, UK) for low-noise (vibration) amplitude and phase determination. The Laser and the photodiode were mounted on micrometer-screw driven positioning tables in order to enable their proper alignment. The SECM tip was stationary, and the electrochemical measuring cell with the sample at the bottom was movable through its fixation on the top of the stage of three joined stepper motors (SPI Robot Systems, Oppenheim, Germany) that had in the *x*-, *y*-, and *z*-direction a nominal resolution of 10 nm per microstep. For the shearforce positioning, the fine displacement in the *z*-direction was achieved with a *z*-piezo cube with a nominal displacement of 100 μm (Physik Instrumente, Waldbronn, Germany). A bipotentiostat (PG 100, Jaissle Elektronik, Waiblingen, Germany) was used to control the electrode potentials and for the current measurement. A chloridized silver wire was used as a pseudo Ag/AgCl reference electrode. To guarantee suitable noise levels, the whole system was placed in a Faraday cage. The software for controlling the entire SECM setup was programmed in Visual Basic 6.0 (Microsoft, Unterschleissheim, Germany). A 16 bit AD/DA board (PCI-2517, Plug-In Electronics, Eichenau, Germany) was used for applying the potentials and for data acquisition. Multidimensional SECM images were constructed from the original data using the imaging software MIRA (Microscopic Image Rapid Analysis, G. Wittstock, Oldenburg, Germany). Origin Pro8 (Origin Lab Corporation, Northampton, MA) served as the tool for line scan display.

RESULTS AND DISCUSSION

Concept of the 4D SF/CD-SECM. Technically, any shearforce-based SECM distance control unit with an optical, piezoelectric, or tuning fork-type quantification of the short-range hydrodynamic tip-to-sample shearforce interactions could be employed for the realization of the proposed 4D SF/CD-SECM concept. The system chosen here comprises a distance control unit based on an optical readout of the shearforces (see Figure 1).

A needle-type, vibrationable carbon fiber microdisk electrode with a high and approved voltammetric sensing quality is attached to the SECM tip holder. Transversal mechanical vibrations at a predetermined resonance frequency are agitated using the piezoelectric tube. The vibration amplitude is made visible by focusing a red laser beam onto the lower end of the glass insulation of the microelectrode and projecting the, thus, generated Fresnel diffraction pattern onto a split photodiode. The difference current of the two segments of the split photodiode is analyzed by a lock-in amplifier with respect to the agitation frequency of the piezoelectric tube. Both the magnitude, R, and the phase shift, Θ, of the photodiode signal can be used as measures of the tip vibration. The signal is continuously followed during the *z*-approach curve. At a predefined threshold value for the change in tip vibration amplitude (e.g., 80% of the value for the freely oscillating tip in bulk solution), the *z*-approach is automatically stopped and the exact *z*-position is recorded.

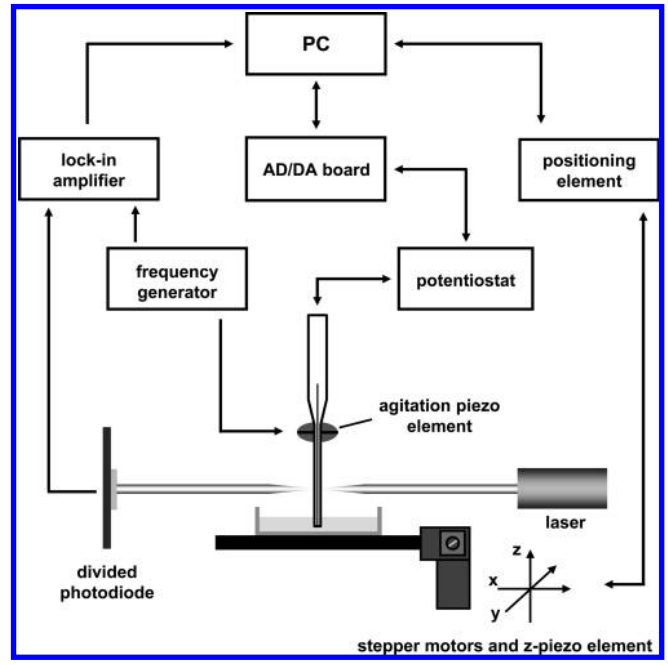

Figure 1. Schematic representation of the instrument setup used for the 4D shearforce-based constant-distance mode of SECM (4D SF/CD-SECM). In all measurements, the SECM tip was a vibrationable disk-shaped carbon fiber microelecrode with a disk diameter of about 7−9 μm. Positioning elements were stepper motors with a nominal resolution of 10 nm per microstep in the *x*-, *y*-, and *z*-direction. To ensure low-noise vibration amplitude monitoring, the lock-in amplifier technique was applied and the reference channel of the instrument was synchronized with the stimulus signal of the piezoelectric actuator. The optical detection of shearforce demands a stationary tip electrode and a movable electrochemical cell with the sample attached to its bottom.

In the conventional shearforce-based constant-distance modes of SECM, this stop criterion would also serve as a set point for the constant-distance feedback loop. Scanning measurements in the common shearforce mode would ensure continuous shearforce interaction between the vibrating SECM tip and the sample surface throughout scanning. As illustrated in Figure 2, the measuring principle of the proposed 4D SF/CD-SECM is different. Here, the threshold value of tip vibration damping is just used to invoke the automatic stop of the *z*-approach, and no feedback loop is started to continuously regulate the tip-to-sample distance in the shearforce regime. When the stop criterion is reached during the approach, the corresponding *z*-position as the closest point of approach is stored together with the tip current as a representation of the sample topography and local electrochemical activity, respectively. The shearforce control is then switched off, and the SECM tip is retracted in predefined *z*-increments. At each newly established, known vertical distance to the sample topography, the tip current is recorded and stored in the computer memory. When the desired number of vertical current measurements are obtained, the SECM tip is moved to the next *x*,*y* grid point, where the sequence of shearforce-controlled tip approach and subsequent stepwise retraction with concomitant current measurements at the same distances above the distance of closest approach is repeated. This procedure leads to a 4D data set containing the SECM tip current response as a function of *x*-, *y*-, and *z*-position of the SECM tip. Different types of 3D plots can be extracted from these 4D raw data. They include a full set of SECM images at different but

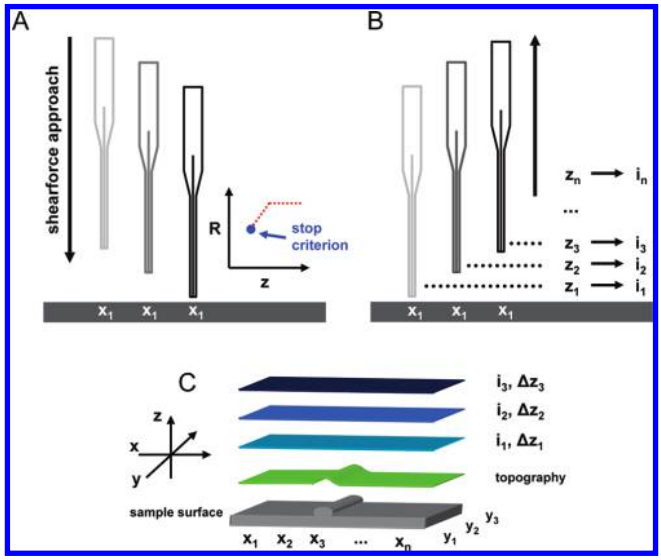

Figure 2. Concept of the 4D shearforce-based constant-distance mode of SECM. (A) An approach of the SECM tip is carried out under optical shearforce control at any *x*,*y* grid point. The tip vibration amplitude changes when the shearforce contact is established and the user can preset a stop criterion for the tip's downward movement. The corresponding readings of the *z*-positioning element (= topography information) and the tip current (= local electrochemical activity) are stored as a function of the *x*,*y*-position. (B) Retraction of the SECM tip for a predefined increment in *z*-direction and subsequent storage of a pair of tip position/tip current values. Repetition of the tip retraction in *z*-direction and the acquisition of the related tip position and current data for a predefined number of times (= distance). (C) The outcome of 4D SF/CD-SECM is a systematic set of *x*,*y*-current images that are valid for different tip-to-topography separations even for distances well outside the shearforce regime.

constant tip-to-sample distances. Since the shearforce topography detection at each grid point is the starting point for all tip retractions, all SECM images are constant-distance images above the sample topography. As a matter of fact, this procedure is not limited to conventional tip amperometry and may be extended to all possible detection modes of SECM including pulse sequences, potentiometry, cyclic voltammograms, etc.

Amperometric 4D SF/CD Feedback-Mode Imaging. A suitable model sample to demonstrate the capability of the proposed 4D SF/CD mode should offer lateral heterogeneity in both topography and local surface conductivity. Thus, we used an array of four Pt microband electrodes fabricated using conventional lithography and lift-off techniques. The sample was examined in an aqueous electrolyte solution containing 100 mM KCl and 5 mM $[Ru(NH_3)_6]^{3+}$ as free-diffusing redox mediator. The carbon-fiber SECM tip was polarized to a potential of −400 mV vs Ag/AgCl to invoke diffusion-limited reduction of $[Ru(NH_3)_6]^{3+}$ to $[Ru(NH_3)_6]^{2+}$ in a feedback-mode configuration, while the four Pt microbands were at open circuit potential (OCP).

Figure 3A shows the shearforce topography image of the Pt microbands as recorded from the *z*-positions of closest approach and automatic stop during the *z*-approach at each grid point. The contours of the four Pt microbands are clearly visible as well as a significant sample tilt in the *y*-direction. Figure 3B−F represents *x*,*y*,*I* plots for five different tip-to-topography separations. The plot in Figure 3B is acquired at the position of closest approach (*d*) and is, hence, comparable with a conventional feedback image in shearforce distance. Since lateral scanning from one grid point to the next is avoided, the risk of tip crash or loosing the shearforce response is unlikely. Moreover, before each shearforce-based *z*-approach, the initial magnitude value of the freely vibrating SECM tip is recorded. Therefore, any possible baseline drift of the shearforce signal does not prevent successful tip positioning. Due to positive feedback at sites above the Pt microband electrodes and negative feedback above the insulator, the local differences in the reaction rate for $[Ru(NH_3)_6]^{3+}$ regeneration are clearly visualized with the best contrast at closest approach. Figure 3C−F contains feedback images obtained at distances of subsequent 5 μm *z*-increments above the position shown in Figure 3A,B. As expected, the feedback contrast fades out with increasing tip-to-sample separation. However, due to the fact that images are recorded in constant distance to the sample topography, the surface tilt as seen in Figure 3A is completely compensated. Essentially, at each *x*,*y*-grid point, a *z*-retraction curve is recorded which could in principle be used for calculating the local electron-transfer rates at the sample surface.

Conventional constant-distance SECM also copes with this demand. However, as pointed out above, shearforce-based constant-distance experiments are often time-consuming and challenging especially if topographies with high aspect ratios or simply large probing areas are involved. Since the tip-to-sample distance has to be kept within the range of the shearforce interaction of only some hundred nanometers, the lateral increments in which the SECM tip could be scanned need to remain very small and the scanning speed slow. Therefore, there are harsh limitations in conventional constant-distance imaging when it comes to coarse-meshed scanning grids. However, even during imaging of smaller sample areas, conventional constant-distance imaging can take a very long time, if the topography features sharp edges, trenches, and holes. These invariably result in a loss of the shearforce set-point value, and further scanning has to wait for incremental feedback readjustment. 4D SF/CD-SECM defeats these disadvantages by means of the repeatedly used shearforce approach curves at each position of the scanning grid.

4D SF/CD Generator/Collector Mode as a Tool for Visualizing Diffusion Profiles. A second proof-of-principle using the proposed 4D SF/CD-SECM mode comprised a Pt disk electrode of 100 μm diameter that was placed upside down in an electrochemical cell containing $[Ru(NH_3)_6]^{3+}$ as free-diffusing redox species. Scanning was done using a carbon fiber disk UME as the SECM tip. The Pt electrode is polarized to a $[Ru(NH_3)_6]^{3+}$ reduction potential while the SECM tip is polarized to a potential suitably high to provoke $[Ru(NH_3)_6]^{2+}$ oxidation. Both potentials were chosen to allow diffusion-limited reaction rate at the tip and sample electrodes. As before, at each point of the scanning grid, the SECM tip electrode is moved downward until the predefined stop criterion expressed as the relative magnitude of the tip-vibration amplitude is attained. The *z*-approach is automatically stopped, the *z*-position is recorded representing sample topography, and the retraction of the tip in predefined increments is initiated while tip position/tip current values are acquired for various distances above the sample surface. As illustrated in Figure 4, a series of SECM images show the topography (A) and five *x*,*y*,*I* profiles

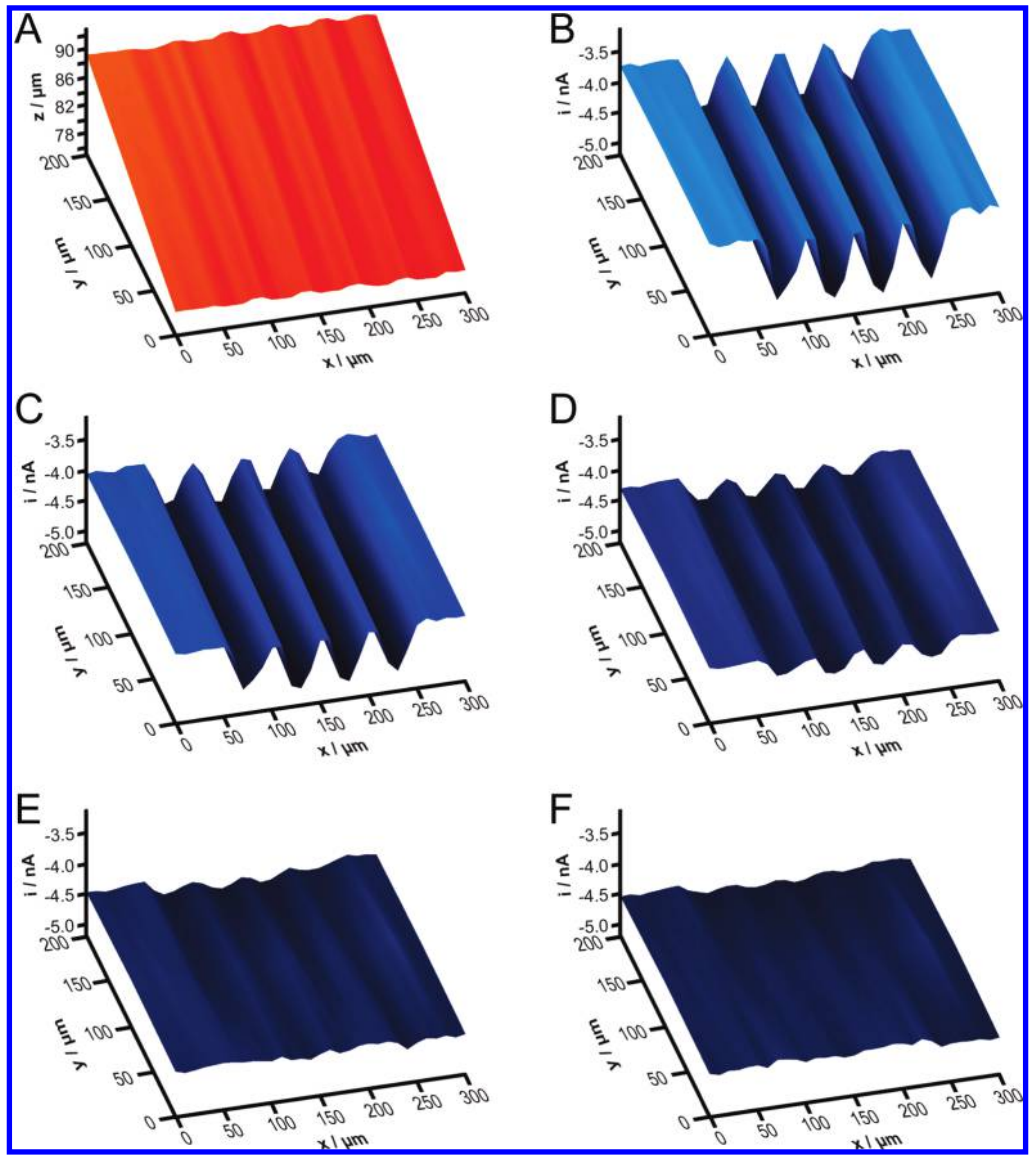

Figure 3. Amperometric feedback mode imaging of a platinum microband array by means of 4D SF/CD-SECM. (A) SECM topography image of the Pt microband array obtained through the *z*-position in shearforce contact vs *x,y* tip position. (B) *x,y,I* image of the SECM amperometric feedback current corresponding to an *x,y* plane situated at the lowest point of tip approach (d). (C−F) *x,y,I* images corresponding to planes that were acquired in 5 μm increments above the plane shown in (B). The parameters for SECM image acquisition were as follows: agitation frequency: 1661 Hz; stop criterion for shearforce approach: change of 20% compared to the value of the lock-in signal in bulk; sample dimensions: four Pt microbands with a width and spacing of 25 μm; bulk electrolyte: 5 mM $[Ru(NH_3)_6]Cl_3$ in 100 mM KCl; SECM tip potential: −400 mV vs Ag/AgCl, sample was at OCP.

(B−F) that are valid for five particular spacings between the SECM tip and the sample at which $[Ru(NH_3)_6]^{2+}$ is generated. The topography image (Figure 4A) shows that the sample is tilted but otherwise flat. The first image (Figure 4B) refers to the data taken at the distance of the preset damping by shearforce interaction (d). The location of the 100 μm diameter Pt disk generator electrode is clearly visible as a bright spot of increased cathodic current. The sharp contrast indicates high collection efficiency for the $[Ru(NH_3)_6]^{2+}$ oxidizing tip electrode. The further images (Figure 4C−F) represent the tip current in planes that are in 5, 10, 15, and 20 μm distances to the sample topography. As expected, the higher the SECM tip was above the specimen, the lower the tip current at grid points above the sample electrode.

In addition to the benefits in terms of the tip movement and the independence from the stability of the shearforce set-point, there is a higher analytical content within the collected data set. As presented in Figure 4, 4D SF/CD SECM can virtually slice the dispersing cloud of $[Ru(NH_3)_6]^{2+}$ that has its origin at the sample electrode and dilutes in all directions via diffusion. This is a straightforward approach to perform diffusion zone imaging experiments outside the shearforce range but in constant tip-to-topography distance.

The 4D data sets as collected in the experiment shown in Figure 4 contain information that can be presented in various different ways. For instance, the tip current as a function of the tip-to-sample separation (*z*-approach curves) can be extracted for selected *x,y* grid points. Figure 5A shows such *I*−*z* curves for two particular grid points. These positions are indicated as white dots in the scheme of the array scan. Position 1 is located above the insulating glass matrix of the sample and position 2 is above the

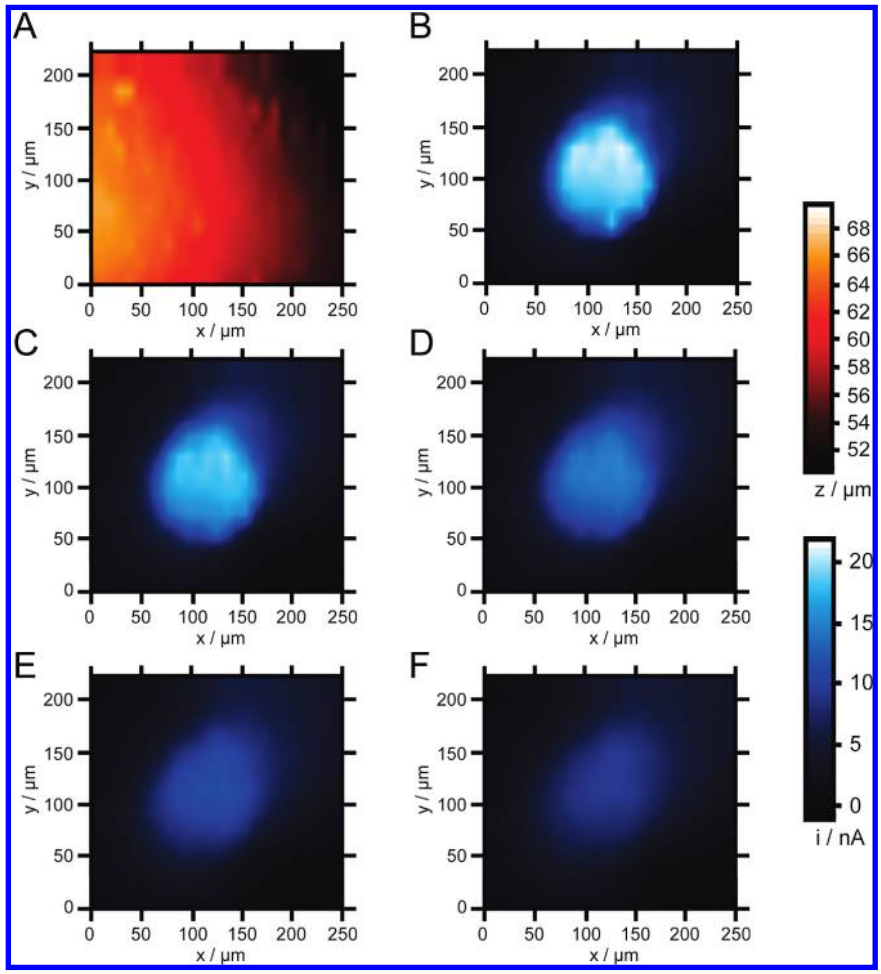

Figure 4. 4D SF/CD-SECM imaging of the diffusion profile of $[Ru(NH_3)_6]^{2+}$ over a Pt disk electrode that actively reduces $[Ru(NH_3)_6]^{3+}$. (A) SECM topography image as revealed from plots of the *z*-piezo position registered in shearforce contact vs *x,y* tip position. (B) *x,y* current SECM image at lowest point of approach (*d*), which is equal to the distance at which shearforce-related tip vibration damping occurred at a user-defined set point value of decrease. (C−F) *x,y* current SECM images corresponding to planes that were acquired in 5 μm increments above the plane shown in (B). The parameters for SECM image acquisition were as follows: agitation frequency: 347 Hz; stop criterion for shear-force approach: change of 5% compared to the value of the lock-in signal in bulk; sample dimension: the polished glass insulated Pt disk electrode that generated $[Ru(NH_3)_6]^{2+}$ from $[Ru(NH_3)_6]^{3+}$ had a diameter of 100 μm and was polarized at −400 mV vs Ag/AgCl; bulk electrolyte: 5 mM $[Ru(NH_3)_6]Cl_3$ in 100 mM KCl; SECM tip potential: 0 mV vs Ag/AgCl.

active Pt surface. The *I*−*z* curve at position 1, which is far away from the area where $[Ru(NH_3)_6]^{2+}$ is formed, shows no differences in the tip current with changes in the tip-to-sample separation. In contrast, a strong dependence of the current signal from the tip-to-sample distances is observed for the *I*−*z* curve at position 2. Higher current values at short distance represent the local higher concentration of the evolving $[Ru(NH_3)_6]^{2+}$ species directly in front of the polarized sample surface. With the full 4D data set at hand, it is also possible to examine line scans in the *x*-direction (*I*−*x* curves), which visualize the distance dependence of the current signal. In Figure 5B, the detected topography as well as the current signals obtained for the point of closest approach (*d*) and for *z*-distances of 10 μm ($d + 10\ \mu$m) and 20 μm ($d + 20\ \mu$m) with respect to this position are shown. The *y*-position of the line scans is chosen across the center of the investigated Pt disk. The topography exhibits a tilt of the sample surface with respect to the scanning plane but is otherwise featureless. The line scan at the distance of the shearforce approach displays the highest contrast between the Pt surface and its insulated surrounding and allows one to assess the sample diameter. A more sophisticated way to present the $[Ru(NH_3)_6]^{2+}$ diffusion zone is realized by construction of *x,z,I* images. These images can be prepared for each *y*-position of the scanned grid and enable one to slice the diffusion cloud vertically, thus displaying how the $[Ru(NH_3)_6]^{2+}$ concentration expands into the bulk of the electrolyte. An *x,z,I* image for a *y*-position in the center of the scanned Pt surface area is shown in Figure 5C.

There may be even processes where free diffusion from or into bulk solution is essential for the imaging experiment. These processes are as a matter of fact not accessible with the conventional shearforce imaging due to scanning at an extremely small tip-to-sample distance. For example, the liberation of metal ions from actively corroding pits may be hindered or at least altered by the close proximity of the tip electrode. The SECM tip and the sample form an electrochemical thin-layer cell. As localized anodic dissolution depends on the actual chemical nature of the environment, pit imaging would benefit from an unhindered diffusional exchange with the bulk solution. Similarly, when inspecting enzyme/polymer structures using disk-shaped SECM

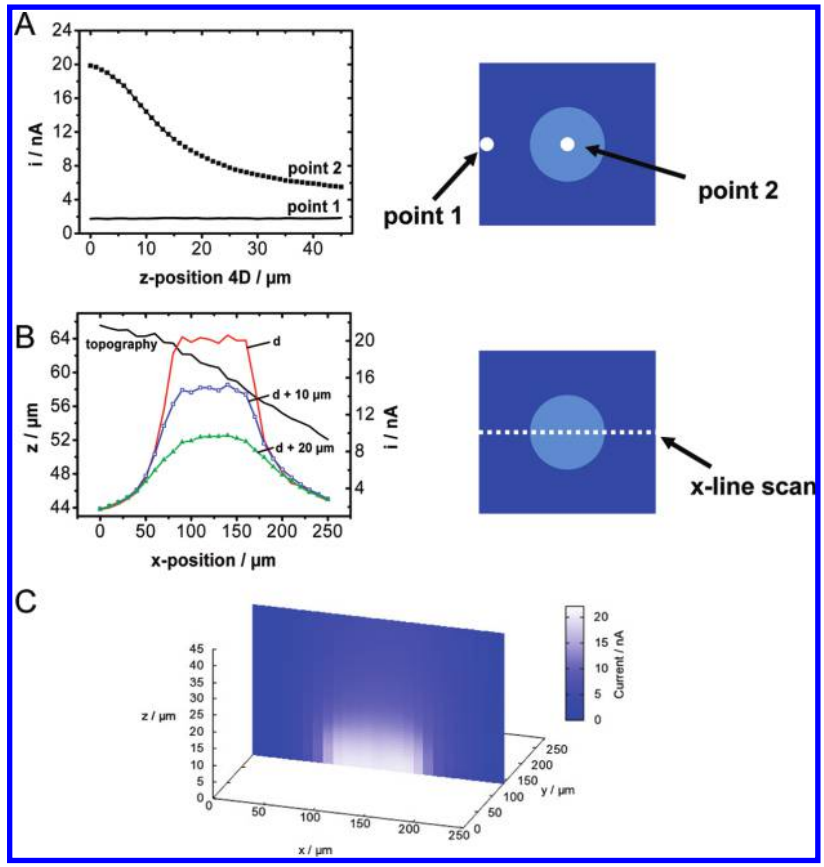

Figure 5. Different data representations extracted from the multidimensional data of the generator/collector experiment displayed in Figure 4. (A) SECM retraction curves at two different grid points: one above the insulating glass surface (point 1) and the other one above the $[Ru(NH_3)_6]^{2+}$-generating Pt disk electrode (point 2). Each curve is constructed from 45 data points in the *z*-direction. (B) SECM line scan starting at positions above glass (dark blue) across the Pt sample electrode (light blue) and to positions above glass again. (C) *x,z,I* image representing the diffusion cloud of the electrochemically produced $[Ru(NH_3)_6]^{2+}$ species at the same *y*-position as in (B).

tips, the substrate transport into the active sites of the enzyme molecules immobilized in the polymer matrix should not be constrained by the closely positioned scanning tip, which, however, should still be close enough for an effective detection of the analytically relevant product of enzyme−substrate interaction. These examples prove an optimum imaging distance may exist, which might well be different from the shearforce interaction range.

CONCLUSION

4D SF/CD-SECM is introduced as a novel tip scanning routine for electrochemical microscopy. It can acquire tip currents at each grid points in planes that are in constant but different distances above the sample topography. The tip-to-topography distances are adjusted by controlled retractions of the SECM tip subsequent to shearforce-based topography detection at each point of the scanning grid. The new SECM mode supports distance-controlled SECM operation without the need of a continuous shearforce interaction between sample and tip throughout scanning. As compared with conventional shearforce scanning of the entire surface topography 4D SF/CD-SECM using a feedback loop for keeping the SECM tip at a *z*-position of constant vibration damping, a lot of time can be saved. Moreover, constant-distance imaging can be carried out at larger *x*- and *y*-increments still decreasing the probability of tip crash. Thus, wide areas and also topographically complex surfaces featuring sharp edges or trenches are now accessible for constant-distance scanning in SECM. The results obtained with 4D SF/CD-SECM measurements are sets of *x,y,I* values that can be compiled and displayed as a function of the *z*-distance from the sample surface. Various images, linescans, or *z*-approach curves can be extracted from the 4D data set. The application of 4D SF/CD-SECM for the visualization of corrosion sites, the local activity of polymer-immobilized enzymes and noble-metal catalysts, and the oxygen-consumption of individual living cells are presently under investigation.

ACKNOWLEDGMENT

M.N. thanks the Ruhr-University Research School funded by Germany's Excellence Initiative for further support [DFG GSC 98/1]. The authors are grateful to the DFG in the framework of the special research area (SFB459, A5).

Received for review April 3, 2010. Accepted August 5, 2010.

AC1008805